Advanced Materials Research Vol. 922 (2014) pp 755-760

doi:10.4028/www.scientific.net/AMR.922.755

The Effects of Heating Rate and Cold Work on the Development of Dual-Phase Steel Microstructures

L.S. Thomas[a], D.K. Matlock[b], and J.G. Speer[c]

Advanced Steel Processing and Products Research Center,

Colorado School of Mines, Golden, CO 80401 USA

[a]lathomas@mines.edu, [b]dmatlock@mines.edu, [c]jspeer@mines.edu

Keywords: Heating rate, recrystallization, austenitization, dual-phase steel

Abstract

The effects of heating rate and prior cold work on the development of dual-phase steel microstructures in three low carbon steels were evaluated with samples processed on a Gleeble 3500 thermomechanical processing simulator. The nominally 0.2 wt pct carbon steels included a plain carbon steel and modified alloys incorporating higher manganese contents, boron additions, and microalloy additions. Each alloy was prepared with two different cold rolled reductions. Heating rates from 1 to 1000 ºC/s were selected to span the rates typically experienced in conventional furnace heat treating up to rates for induction heating. Critical transformation temperatures were obtained from dilatometric curves. Dual-Phase microstructures after heat treatment with different heating rates were compared. Transformation temperatures decreased with an increase in cold work and increased with an increase in heating rate. The steels with higher manganese and carbon additions exhibited lower Ac_3 values across all heating rates and the steels with higher silicon higher Ac_1 temperatures across all heating rates. Ac_1 increased less than Ac_3 with increasing heating rate. The increase in transformation temperatures between 100 and 1000 °C/s was smaller than values exhibited over other increments in heating rate, and decreased in one steel; contributing factors were identified for this behavior.

Introduction

High heating rates are of interest for annealing dual-phase (DP) steels in some applications. Heating rates in excess of 1000 ºC/s can be achieved through a variety of methods such as induction, electric, direct resistance, or flame. Current continuous annealing lines for dual-phase steels typically have heating rates of 5-10 ºC/s, but some applications may employ much higher rates [1]. As heating rates increase, effects of heating rate on DP steels become more important. Reports of testing at heating rates above 100 °C/s in DP steels are still relatively recent. Comparisons between steels with different alloy contents and processed with different heating rates are also rare for this class of steels [2]. While microstructural comparisons between hot-rolled (HR) and cold-rolled (CR) steels heat treated after different heating rates to intercritical annealing temperature have been performed [2, 3], complete comparisons between two different cold reductions have not previously been reported. Attempts at modeling the effects of heating rate on transformation temperature are limited and those that have been reported predict a linear increase in transformation temperature with heating rate [4].

Transformation temperatures change with increasing heating rate because less time is available for diffusion. Ac_1 and Ac_3 temperatures are typically reduced through cold rolling, which also reduces the sensitivity of increases in transformation temperature with increasing heating rate [3]. In CR ferrite-pearlite steels multiple processes occur during continuous heating: recovery, recrystallization, spheroidization of pearlite, growth of ferrite grains, and austenite formation [5]. Heating rates also influence the precipitation and coarsening of important precipitates such as AlN and NbC. Recrystallization is controlled by degree of cold work, heating rate, and alloy content [2]. At low heating rates, recrystallization and spheroidization have sufficient time to complete before austenite formation starts. Greater cold work increases the driving force for recrystallization, and so

recrystallization occurs more quickly. Austenite nucleates at ferrite-ferrite grain boundaries or ferrite-cementite boundaries. Spheroidization reduces the number of sites available for austenite nucleation. At higher heating rates, recrystallization may still occur even after austenite formation starts, influencing the kinetics of austenite nucleation and growth, and the character of available nucleation sites. Growth of austenite after nucleation at ferrite-cementite boundaries then occurs most quickly into the pearlite bands, leading to more banded martensite structures after cooling from the intercritical region. After cementite dissolution, austenite formation is primarily controlled by austenite growth into ferrite by carbon diffusion [6]. At the end of austenite transformation, there is a rapid transformation of the final ferrite grains to austenite [7]. Therefore, the purpose of this paper is to study austenite formation and recrystallization with different heating rates and cold reduction and the effects on resulting dual-phase steel microstructures.

Experimental Procedure

Three nominal 0.2 wt pct (C) steels, 1020, 1019M, and 15B25, were tested. The 1020 steel was a carbon and manganese steel (0.2C-0.5Mn), the 1019M was modified with increased Mn and a niobium addition (0.17C-1Mn-0.01Nb), and the 15B25 steel included more complex microalloying additions and boron (0.25C-1.2Mn-0.23Si-0.53Cr-0.02Ni-0.036Ti-0.03Nb-0.0011B) (all compositions in wt pct). Two different cold reductions (CR) were performed. These included a low cold reduction (referred to as LCR) of nominally 40% and a high cold reduction (referred to as HCR) of nominally 60% in thickness by rolling. The actual cold reductions for these steels was 39 and 59% for the 1020 steel, 41 and 53% for the 1019M steel, and 33 and 58% for the 15B25 steel. Each steel condition is referred to by cold reduction and alloy designation, e.g. LCR 1020 is SAE 1020 with 39 pct cold reduction.

Dilatometry measurements were obtained with a Gleeble 3500 where dimensional changes were measured with a non-contact laser dilatometer transverse to the rolling direction. Gleeble 3500 samples used a sample free span of 15 mm, width of 6 mm, and specimen thickness of 1-2 mm. Samples were machined with the length in the rolling direction. Tests were performed at 1, 10, 100, and 1000 °C/s. Three or more tests were performed for each condition. Standard procedures for laser dilatometry were followed for each test condition. Transformation temperatures of Ac_1 and Ac_3 were found from analysis of the dilation curves. Figure 1 shows the analysis of dilation curves at 1 and 1000 °C/s using HCR 1020. Ac_1 is found at the point where the dilation line deviates from linearity. Ac_3 is then achieved when the new line (austenite) is reached. Ac_{1f}, the pearlite-to-austenite finish temperature, is visible with low heating rates but not with high heating rates, so that temperature was not determined. Specimens were also intercritically annealed to characterize partially transformed microstructures.

Results and Discussion

Measured transformation temperatures are summarized in Table 1. In general Ac_1 and Ac_3 increased with increasing heating rate. Ac_3 generally increased more than Ac_1. The lesser cold worked samples had a greater increase in transformation temperatures with increasing heating rate, although deviations in this behavior were sometimes observed. The increase in Ac_1 with increasing heating rate was smaller with the HCR condition, however. The 15B25 steel had lower transformation temperatures across the range of heating rates with greater cold work. The increase in transformation temperatures for all steels and conditions between 100 and 1000 °C/s is smaller than observed over the other increments of heating rate, and smaller than reported previously [3]. In fact, for both the LCR and HCR conditions, the 15B25 steel exhibited an apparent *decrease* in Ac_1 and Ac_3 between 100 and 1000 °C/s.

Figure 2 presents a series of micrographs for cold-rolled and intercritically annealed conditions. Figures 2a-2b show cold-rolled 1019M in the LCR (Fig. 2a) and HCR (Fig. 2b) conditions. Figures 2c-2e compare plain carbon (1020) and micro-alloyed (1019M) steels at the lowest (1 °C/s) and highest (1000 °C/s) heating rates tested. Each sample was held for 10 s at

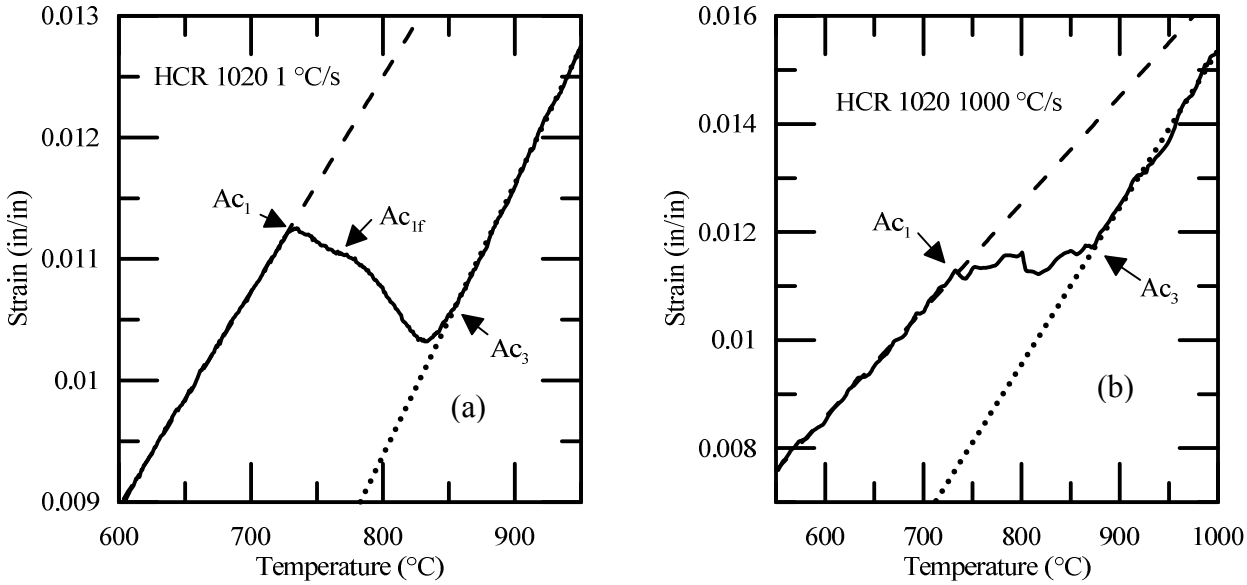

Figure 1 Dilation curves (strain vs temperature) for HCR 1020 at heating rates of 1 °C/s (a) and 1000 °C/s (b). Ac_{1f} (the pearlite-to-austenite finish temperature) is visible at low heating rates but not discernible at high heating rates. Ac_1 is the point where the line deviates from linearity, and Ac_3 is the point at which the curve returns to linearity.

Table 1 – Transformation Temperatures for Each Steel and Cold Reduction

Steel	Transformation	1 °C/s	10 °C/s	100 °C/s	1000 °C/s
LCR 1020	Ac_1	732 ± 4	733 ± 3	739 ± 5	747 ± 6
	Ac_3	853 ± 4	861 ± 5	878 ± 5	882 ± 2
HCR 1020	Ac_1	730 ± 1	730 ± 2	741 ± 4	741 ± 3
	Ac_3	856 ± 2	866 ± 4	880 ± 5	883 ± 4
LCR 1019M	Ac_1	730 ± 4	735 ± 3	737 ± 3	740 ± 5
	Ac_3	860 ± 4	860 ± 1	873 ± 4	881 ± 8
HCR 1019M	Ac_1	728 ± 2	729 ± 4	737 ± 3	740 ± 3
	Ac_3	859 ± 4	860 ± 1	872 ± 4	875 ± 9
LCR 15B25	Ac_1	742 ± 3	754 ± 4	771 ± 3	768 ± 3
	Ac_3	836 ± 2	857 ± 5	872 ± 5	860 ± 4
HCR 15B25	Ac_1	743 ± 4	751 ± 4	754 ± 4	752 ± 3
	Ac_3	839 ± 4	851 ± 5	857 ± 4	855 ± 6

770 °C. The cooling rate was nominally 70 °C/s for each condition. Samples held for less than 1 s had similar microstructural features to those held for 10 s. All micrographs were taken on the cross-section containing ND-RD orientations on samples etched with 2% nital. Figures 2a-2b show the reduction in pearlite band width with greater cold reduction. Greater cold work increases the driving force for recrystallization, so it occurred at lower temperatures as CR increased, see Figs. 2d-2e. Figure 2d is HCR 1019M heated at 1 °C/s and Fig. 2e is LCR 1019M heated at 1 °C/s. Figure 2e (LCR 1019M) shows evidence of unrecrystallized grains from a combination of equiaxed, "clean" grains and pancaked, deformed grains [8]. The HCR 1019M (Fig. 2d) does not have these characteristics because of the increased driving force for recrystallization, so recrystallization was more complete before austenite formation began. LCR 1020 (Fig. 2c), though only receiving 39% cold reduction, was fully recrystallized, presumably because this alloy had fewer microalloy

carbonitrides to retard recrystallization. Martensite banding is observed in the DP steels at high heating rates as shown in Fig. 2f. This observation is consistent with previous studies [2].

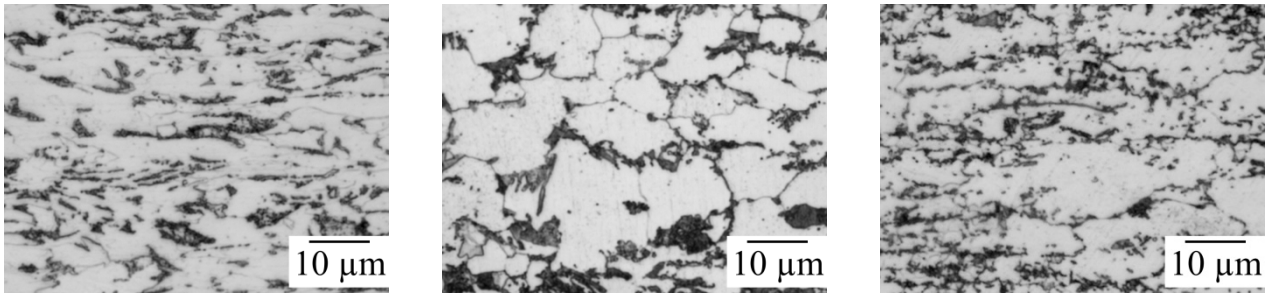

(a) LCR 1019M Cold-Rolled (c) LCR 1020 1 °C/s (e) LCR 1019M 1 °C/s

(b) HCR 1019M Cold-Rolled (d) HCR 1019M 1 °C/s (f) HCR 1019M 1000 °C/s

Figure 2 As received LCR 1019M (a) and HCR 1019M (b). 770 °C intercritical anneal for 10 s (c-f), 1 °C/s (c-d), 1000 °C/s (e-f). Etched with 2% nital. ND-RD orientation.

For all evaluated alloys and cold work conditions Ac_1 generally increased less than Ac_3 with increasing heating rate. This behavior is explained by two primary factors. First, the start of austenite nucleation is controlled by short-range diffusion [6], which is largely independent of heating rate. Second, at high heating rates there is less spheroidization and therefore many sites available for austenite nucleation [9], mitigating the increase in the Ac_1 temperature. It was found that Ac_3 increased between 1 and 100 °C/s, but the increase was smaller between 100 and 1000 °C/s. The data in Table 1 also show that a slight decrease in Ac_3 was observed in both LCR and HCR 15B25.

Figure 3 shows comparisons of dilation curves of 100 and 1000 °C/s for LCR 15B25 (Fig. 3a) and HCR 15B25 (Fig. 3b). It can be seen that Ac_3 is reached at similar or lower temperatures with a heating rate of 1000 °C/s than as was reached with 100 °C/s. The reason the Ac_3 temperature was lower at high heating rates is difficult to determine. The deviation from expected behavior may be related to recrystallization. At higher heating rates recrystallization is completed at higher temperatures during continuous heating. Therefore, the stored energy in the unrecrystallized ferrite is available to help drive austenite formation, and the recrystallized ferrite grains are smaller with higher heating rates because the grains have had little time for growth. It is possible that Ac_3 is reduced at 1000 °C/s because of the greater driving force and the greater grain boundary area (due to smaller grain size) that provides nucleation sites in the final period of austenitization. This may cause the final, rapid transformation of ferrite to austenite to occur at lower temperatures.

Another possible explanation for the reduction, or smaller than expected increase, of Ac_1 and Ac_3 between 100 and 1000 °C/s is the presence of retained austenite in the starting microstructure. In steels with retained austenite the austenite decomposes during heating before transformation. Austenite therefore has to nucleate before growth. At higher heating rates the austenite does not have time to decompose and growth of existing austenite starts at lower temperatures because nucleation does not have to occur. This transition was found above 100 °C/s [10]. While the steels studied here were not expected to have large fractions of retained austenite, it may be that the small

fraction of retained austenite was sufficient affect the start of transformation. The steel with the highest amount of austenite stabilizing elements, 15B25, is the steel with a reduction of Ac_1 and Ac_3 between 100 and 1000 °C/s. Further study is required to explain this observed behavior, and to rule out possible testing issues at high heating rates.

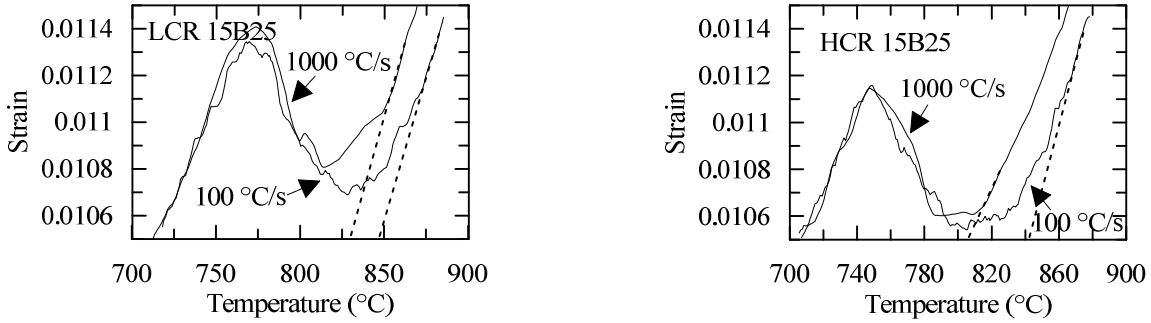

(a) (b)

Figure 3 Comparison of dilation curves of LCR 15B25 (a) and HCR 15B25 (b). The end of austenite transformation before Ac_3 is slower at 100 °C/s than 1000 °C/s.

Alloying affects Ae_1 and Ae_3. Alloying effects with changing heating rate have received minimal study. Predictions of transformation temperatures based on compositions are complex, and many different models are available. The simplest method is a linear regression in transformation temperature with each composition change from pure iron. The classic example of a linear regression is the Andrews equation [11]. Linear models assume that change in transformation temperatures are additive, and do not account for interactions between elements or prior-microstructure effects. Furthermore, the Andrews equation is limited to a small number of elements and compositional ranges. An example of a more complex model is due to Kasatkin and Vinokur [12], which takes into account statistical interactions between alloy elements.

A summary of values calculated using both the Andrews and Kasatkin-Vinokur models is provided in Table 2. Neither of these models includes prior microstructure, cold work, or heating rate. The Andrews equation was determined using a heating rate of 0.125 °C/min. Kasatkin and Vinokur did not state what heating rate was used. Measured values from the LCR condition are compared to the calculations, as they are most similar to the hot-rolled steels used to develop the models. The lowest heating rate, 1 °C/s, was used because it is closest to equilibrium. The more complex model is closer to the measured values. On average the Andrews model predicts values that are 16 degrees lower for Ac_1 and 26 degrees lower for Ac_3 than for the experimental measurements. The Kasatkin and Vinokur model is, on average, 14 degrees lower for Ac_1 and 8 degrees lower for Ac_3. If the models incorporated heating rate, or if even lower heating rates were tested, the measured values would likely be closer to the models. In general, the measured values are similar to those predicted by the equations. The 1019M and 1020 steels have similar Ac_3 transformation temperatures at 1 °C/s, but 1019M has lower Ac_3 temperatures at higher heating rates. This difference is likely due to heating rate effects discussed above. The 15B25 steel has the lowest Ac_3 temperatures at all heating rates; 15B25 was also calculated to have the highest Ac_1, which is observed across all heating rates.

Conclusions

Cold work reduces Ac_1 and Ac_3 across all heating rates measured. Transformation temperatures increase as heating rate increases. The increase was smaller than between 100 and 1000 °C/s, and a *decrease* was observed in 15B25 steel over this range of heating rates. The Ac_1 increase is much less than Ac_3 with increasing heating rate. At high heating rates austenite nucleates at pearlite, and starting microstructure (retained austenite and microalloy precipitation) and recrystallization behavior may contribute to differences in the austenite transformation kinetics. Basic alloying effects (such as C, Mn, Si) on Ac_1 and Ac_3 were found to remain with changing heating rate, though other effects can dominate with high heating rates.

Table 2 – Summary of Measured and Calculated Transformation Temperatures

Test/Calculation	Ac1 (°C)	Ac3 (°C)
LCR 1020 1 °C/s	732	853
1020 Andrews	718	820
1020 Kasatkin and Vinokur	721	844
LCR 1019M 1 °C/s	730	856
1019M Andrews	713	827
1019M Kasatkin and Vinokur	717	845
LCR 15B25 1 °C/s	742	836
15B25 Andrews	725	819
15B25 Kasatkin and Vinokur	724	831

Acknowledgments

The authors acknowledge the support of the Advanced Steel Processing and Products Research Center, an Industry-University Cooperative research center at the Colorado School of Mines. Tube Investments of India Ltd. is acknowledged for providing the experimental cold-rolled material.

References

[1] P. Shanmugam, K. Srinivas, M. Preethi, and R. Natarajan, "Development of Ductile Martensitic Tubes and its Application in Automotive Parts," *1st Conference on Super High Strength Steels,* 2-4 Nov. 2005, Italy.
[2] J. Huang, W.J. Poole, and M. Militzer, "Austenite Formation During Intercritical Annealing," *Metallurgical and Materials Transactions A,* vol. 35, Nov. 2004, pp. 3363-3375.
[3] H. Azizi-Alizamini, M. Militzer, and W.J. Poole, "Austenite Formation in Plain Low-Carbon Steel," *Metallurgical and Materials Transactions A,* vol. 42, Dec. 2010, pp. 1544-1557.
[4] F. G. Caballero, C. Capdevila, and C. G. D. E. Andrés, "An Attempt to Establish the Variables That Most Directly Influence the Austenite Formation Process in Steels," *ISIJ International*, vol. 43, no. 5, pp. 726–735, 2003.
[5] D.Z. Yang, E.L. Brown, D.K. Matlock, and G. Krauss, "The Formation of Austenite at Low Intercritical Annealing Temperatures in a Normalized 0.08C-1.45MN-0.21Si Steel," *Metallurgical Transactions*, vol. 16, 1985, pp. 1523-1526.
[6] G.R. Speich, V.A. Demarest, and R.L. Miller, "Formation of Austenite During Intercritical Annealing of Dual-Phase Steels," *Metallurgical Transactions A*, vol. 12, Aug. 1981, pp. 1419-1428.
[7] C. G. de Andrés and F. Caballero, "Application of Dilatometric Analysis to the Study of Solid–Solid Phase Transformations in steels," *Materials Characterization*, vol. 48, pp. 101–111, 2002.
[8] T. Ogawa, N. Maruyama, N. Sugiura, and N. Yoshinaga, "Incomplete Recrystallization and Subsequent Microstructural Evolution during Intercritical Annelaing in Cold-rolled Low Carbon Steels, *ISIJ International,* vol. 50, no. 3, pp. 469-475, 2010.
[9] D. San Martín, Y. Palizdar, C. García-Mateo, R. C. Cochrane, R. Brydson, and A. J. Scott, "Influence of Aluminum Alloying and Heating Rate on Austenite Formation in Low Carbon-Manganese Steels," *Metallurgical and Materials Transactions A*, vol. 42, no. 9, pp. 2591–2608, Apr. 2011.
[10] L. Gavard, H. K. D. H. Bhadeshia, C. Mackay, and S. Suzuki, "Bayesian Neural Network Model for Austenite Formation in Steels," *Materials Science and Technology*, vol. 12, no. June, pp. 453–463, 1996.
[11] K.W. Andrews, "Empirical Formulae for the Calculation of Some Transformation Temperatures," *JISI,* vol. 203, 1965, pp. 721-727
[12] O. Kasatkin, B. Vinokur, and V. Pilyushenko, "Calculation Models for Determining the Critical Points of Steel," *Metal Science and Heat Treatment,* vol. 26, no. 1, pp. 27–31, 1984.